Available online at www.sciencedirect.com

ScienceDirect

journal homepage: www.elsevier.com/locate/he

Nafion–titanate nanotubes composites prepared by *in situ* crystallization and casting for direct ethanol fuel cells

B.R. Matos [a,*], R.A. Isidoro [a], E.I. Santiago [a], A.C. Tavares [c], A.S. Ferlauto [b], R. Muccillo [a], F.C. Fonseca [a]

[a] Instituto de Pesquisas Energéticas e Nucleares, IPEN, Av. Prof. Lineu Prestes, 2242, São Paulo, SP 05508000, Brazil
[b] Universidade Federal de Minas Gerais, Departamento de Física, UFMG, Avenida Antônio Carlos, 6627, Belo Horizonte, Minas Gerais 31270901, Brazil
[c] Institut National de la Recherche Scientifique, Énergie, Matériaux et Télécommunications, INRS-EMT, 1650 Boulevard Lionel-Boulet, Varennes, Québec J3X 1S2, Canada

ARTICLE INFO

Article history:
Received 21 October 2014
Received in revised form
13 November 2014
Accepted 18 November 2014
Available online 17 December 2014

Keywords:
Direct ethanol fuel cell
Nafion
Composite
Water retention

ABSTRACT

The physical properties relevant for the application of Nafion–titanate nanotubes composites in electrochemical devices such as water absorption capacity, ion conductivity, and thermal stability are reported. The nanocomposites were prepared by *in situ* hydrothermal conversion of anatase into titanate nanotubes in Nafion matrix and by casting of nanotube suspensions in Nafion. Composites were characterized by differential scanning calorimetry (DSC), dynamic vapor sorption (DVS), X-ray diffraction (XRD), transmission electron microscopy (TEM), proton conductivity, and tested in direct ethanol fuel cells (DEFC). Nafion–titanate nanotubes displayed higher water retention capacity in comparison with Nafion–titania composites as revealed by DSC and DVS. The ion conductivity at intermediate temperatures (80–130 °C) for Nafion–titanate nanotube composites is higher than Nafion–titania composites indicating that the hydrophilicity and conduction properties of the titanate phase contributed to the improvement of the membrane electrical properties. The Nafion–titanate nanotube composites prepared by *in situ* sol–gel exhibited improved electric and electrochemical performance at high temperatures compared to the composite prepared by casting. The combined XRD, DSC, and TEM data indicated that at $RH = 100\%$ Nafion–titanate nanotubes are thermally stable up to 130 °C, but for higher temperatures the titanate nanotubes are converted to rutile nanorods.

Introduction

Direct ethanol fuel cells (DEFCs) have been considered to be cleaner and more efficient energy converters as compared to conventional fossil-fueled devices [1–3]. However, several drawbacks such as short-term durability of DEFCs components, high ethanol crossover through the polymer electrolyte, and sluggish ethanol oxidation and oxygen reduction

* *Corresponding author.*
E-mail address: brmatos@usp.br (B.R. Matos).
http://dx.doi.org/10.1016/j.ijhydene.2014.11.102

reactions severely reduce their conversion efficiency. Such hurdles have postponed the commercialization of this type of fuel cell [1]. One approach to improve the DEFC performance is to increase the operating temperature and lifetime by replacing the traditional polymer membrane for a mechanically robust and a high-proton conducting electrolyte [4,5].

The proton conductivity in hydrated Nafion membranes is strongly dependent on the dynamics of absorbed water molecules [6–8]. At 80 °C and high relative humidity ($RH = 100\%$), Nafion exhibits high proton conductivity as a result of the predominant structural diffusion over the vehicular transport of protons in the electrolyte [9]. Such feature results in high power density outputs in polymer electrolyte fuel cells running on hydrogen [2]. In addition, perfluorosulfonate ionomers, such as Nafion, are known to have superior thermomechanical properties and chemical stability when compared to conventional polymers [8,10]. However, Nafion membranes have a high permeability to alcohol fuels such as methanol and ethanol, which decreases dramatically the fuel cell efficiency due to the alcohol oxidation reaction at the cathode [1,2,4,5]. Moreover, such solvent molecules act as plasticizers thereby reducing the mechanical stability of ionomer electrolytes during fuel cell operation [11].

The DEFC operation without appropriate electrocatalysts and at a low temperatures is hindered by incomplete ethanol oxidation that results in the formation of substantial amounts of by-products such as acetic acid and acetaldehyde [12–14]. Several studies have concentrated on the development of new electrocatalysts to improve ethanol oxidation and increase the DEFC efficiency [12–14]. It has been demonstrated that efficient operation of DEFC is attained in the 110–130 °C temperature range by using high-performance electrocatalyst alloys [12–14]. More recent results have shown that the efficiency of DEFC, using Polybenzimidazole (PBI) electrolytes and electrocatalysts based on Platinum alloys, increases as the operation temperature increases in the 130–260 °C range [15,16]. Thus, the increase of DEFC operation temperature has been a subject of great interest for increasing the ethanol oxidation efficiency, while enhancing the both water and heat managements of the device [17]. However, fewer studies have dedicated to tailor new electrolyte membranes in order to increase the DEFC efficiency. The increase of the operation temperature is limited by the standard polymeric electrolyte (Nafion), which, in its pristine form, does not possess the thermal stability and the water retention necessaries to sustain high temperature conditions [5]. Indeed, to increase the DEFC temperature above 100 °C has been a hard task. As an alternative, PBI membranes with high thermal stability and high proton conductivity at high temperatures have been used as electrolytes allowing the operation of DEFC at higher temperatures [15,16]. However, PBI membrane shares some common deficiencies with Nafion, such as ethanol crossover and the reduction of the proton conductivity due to the leaching out of the charge carriers, which drastically reduces the DEFC performance [18]. The performance of fuel cells directly fed with alcohols using different electrolyte such as solid acid proton conductors ($T \sim 243$ °C) [19,20] and PBI ($T \sim 200$ °C) [15] and Nafion based composites ($T \sim 130$ °C) [4,5,27] the reported power densities are of the order of ~ 35 mW cm^{-2}, ~ 10–60 mW cm^{-2} and ~ 20–50 mW cm^{-2}. In this framework, the increase of the DEFC efficiency cannot be only met by increasing the operation temperature and must be accompanied by the development of electrolyte materials with low fuel crossover, low thickness, high and stable proton conductivity at high temperature [21–24].

In order to overcome such limitations, the addition of inorganic hydrophilic fillers (TiO_2, SiO_2, etc) to Nafion has been considered. However, such materials have relatively low superficial ion conductivity (~10^{-4} S cm^{-1}) and, thus, significant reductions in the proton conductivity of the composite membranes are usually observed [4,26]. In this sense, the use of proton conducting fillers such as titanate nanotubes ($H_2Ti_3O_7 \cdot nH_2O$) can improve the mechanical stability and lower the alcohol permeability without drastically reducing the conductivity of the composite [26,27]. Recently-developed titanate nanotubes have high specific surface area, high hydrophilicity, and high proton conduction at high relative humidity (~10^{-2} S cm^{-1}–10^{-3} S cm^{-1}), thus good candidates to be used as fillers in Nafion membranes [28].

In a previous report, we showed that the Nafion–titanate nanotube composites, prepared *in situ* by the crystallization of 1D structures directly inside Nafion, have enhanced properties with respect to Nafion–titania composites that resulted in a significant boost of DEFC performance at 130 °C [27]. However, DEFC performance at high temperatures has been associated with different parameters, such as thermal stability, morphology, water retention, ethanol crossover, and proton conductivity [4]. Thus, the present study investigates the influence of the synthesis method on relevant properties of composite electrolytes, such as thermal stability and water absorption and retention capacities. These properties directly affect the proton conductivity and fuel cell performance and are relevant to advance the understanding of Nafion-based composite electrolytes.

Experimental

Membrane synthesis

Titania (TiO_2) nanofillers in acid Nafion membranes (N115/H) were prepared *in situ* by the sol–gel method. The methodology consisted of the controlled hydrolysis of titanium tetraisopropoxide embedded in Nafion commercial membranes (N115) using a hydrogen peroxide solution [29]. The resulting Nafion–titania (N–TiO) composite membranes were washed and protonated [29]. For the titania to titanate nanotubes conversion, the N–TiO composite membranes (4 × 4 cm^2) were immersed in 50 mL of a concentrated basic solution (NaOH/10 mol L^{-1}) and placed inside a Teflon covered stainless steel reactor. A microwave-assisted hydrothermal process was performed by placing the reactor in a microwave oven at 140 °C for 180 min. The resulting Nafion–titanate nanotubes membranes in the sodium form ($Na_2Ti_3O_7 \cdot nH_2O$ – N-TN/Na) were copiously washed with distilled water at 70 °C to remove excess of sodium hydroxide. Ion exchange was carried out overnight at room temperature to convert the membranes to the proton form ($H_2Ti_3O_7 \cdot nH_2O$ – N-TN/H) by immersing the N-TN/Na in a 400 mL dilute solution of HCl (0.1 mol L^{-1}) and subsequently washed with distilled water to remove excess of chemicals. The N-TN composite samples in the proton and sodium forms were synthesized with volume fractions of ~ 16 vol% and ~ 15 vol%,

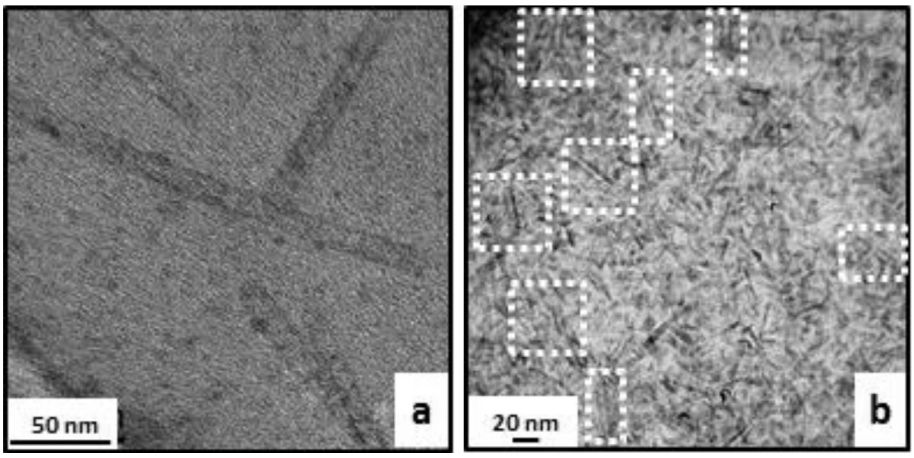

Fig. 1 – Representative TEM images of (a) Nafion–titanate nanotubes prepared by casting in the proton form (~5 vol%); (b) Nafion–titanate nanotubes prepared by the hydrothermal synthesis in the sodium form (~16 vol%). The dashed rectangles enclose some of the observed nanotubes.

respectively. A Nafion–titania (~15 vol%) in the sodium form (N-TiO/Na) prepared by sol–gel and two Nafion–titanate nanotubes (N-TN/Hcast) composites (~5 vol% and 15 vol%) prepared by casting were used for comparison purposes. N–TiO/Na samples were obtained by immersing the composite in 1.0 mol L^{-1} NaOH solution for 1 h at 80 °C and subsequently washed with deionized water, this step was repeated three times to assure a high degree of conversion. N-TN/Hcast samples were prepared by following a previously reported procedure [30,31]. The final thicknesses of the dry membranes for N115/H, N–TiO/H (and N–TiO/Na) and N-TN/H (and N-TN/Na) are 131 μm, 152 μm, and 159 μm, respectively.

Membrane characterization

Transmission electron microscopy (TEM) images were recorded using a JEOL-2100F instrument with 100–200 kV of applied voltage on thin films (<100 nm) prepared with an ultramicrotome in the plane direction of the film. For the dynamic water sorption (DVS) experiments, a DVS – High Throughput apparatus (Surface Measurement Systems, London, UK) equipped with a Cahn ultramicrobalance with a mass resolution of 10 μg was used. Typically 10 mg of sample were placed into the DVS-HT pans and dried under a stream of dry N_2 at 25 °C for 3 h. After the initial drying step, samples were successively exposed to a relative humidity (*RH*) square function in the range $RH = 0–98\%$ with a $RH_{step} = 10\%$. At each *RH* step the water uptake during sorption and desorption were collected in a period of 6 h. The diffusion coefficient of water (*D*) was estimated from the sorption curves and by adjusting the linear portion of the $M(t)/M(\infty)$ vs $t^{1/2}$ plots, where $M(t)$ is the time dependence of water uptake and $M(\infty)$ is the water uptake at equilibrium at a fixed *RH*. By assuming a Fick diffusion with constant diffusivity and knowing the initial membrane thickness (*d*) the *D* values were obtained with the following equation [25,32]:

$$D = \left(\frac{M(t)}{M(\infty)}\right)^2 \frac{\pi d^2}{16t} \quad (1)$$

Differential scanning calorimetry (DSC) was performed from −50 °C to 250 °C with a heating rate of 20 °C min^{-1} under N_2 flow.

Proton conductivity was measured by impedance spectroscopy (IS) using a frequency response analyzer (Solartron 1260) and a homemade Teflon sample holder with stainless steel terminal leads and a K-type thermocouple [33]. For IS measurements, samples were sandwiched between carbon cloth electrodes in order to facilitate the equilibrium with water vapor. The sample holder was inserted in an airtight stainless steel chamber containing distilled water to ensure $RH = 100\%$ during measurements. Two-probe (through-plane) IS measurements were performed in the 20–180 °C temperature range, in the 0.01 Hz–30 MHz frequency interval, with 100 mV applied amplitude [33].

Nafion and composite membranes were evaluated in 5 cm^2 single fuel cells. The anode was prepared with PtSn/C (Pt:Sn of 75:25 Etek) and Nafion loadings of 1.0 mg cm^{-2} and 30 wt%, respectively. The cathode is composed of Pt/C and Nafion loadings of 1.0 mg cm^{-2} and 30 wt%, respectively. The single cell was fed with 1.0 mol L^{-1} ethanol solution and 5.0 mL min^{-1} flow rate at the anode at 1 atm and with pure oxygen at the cathode at 3 atm absolute pressure. Fuel cell and oxygen humidifier temperatures were varied from 80 °C to 130 °C. Polarization curves were obtained in duplicate experiments with estimated error of ~10% in the 80 °C–130 °C temperature range.

X-ray diffraction (XRD) measurements were performed with Rigaku-Miniflex II diffractrometer with Cukα radiation ($\lambda = 1.54$ Å) in the 2θ range of 5–80°.

Results and discussions

Fig. 1 shows representative TEM images of N-TNcast (Fig. 1a) and *in situ* N-TN composites (Fig. 1b) containing ~ 5 vol% and ~ 16 vol% of the inorganic phase, respectively. Both organic and inorganic phases are unstable under the high energy electron beam making higher magnification images difficult to be

obtained. Although there is a relatively low contrast between the nanotube wall and the polymeric matrix, it is possible to distinguish in the TEM micrographs the *ex situ* prepared titanate nanotubes added to Nafion in cast composites (Fig. 1a). In Fig. 1b, it is possible to observe a large amount of hollow elongated nanostructures evidencing the existence of nanotubes in the *in situ* N-TN composite.

In Fig. 1b, coexisting titanate nanotubes and nanorods are evidenced. The presence of nanorods can be attributed to titanate nanostructures that failed to fold into the nanotubular form in the constrained polymer structure. Indeed, nanorods and nanosheets have been observed in the *ex situ* synthesis of titanate nanotubes [34].

The superior electrical and mechanical properties of *in situ* N-TN compared to N-TNcast can be associated to the different morphologies resulting from the distinct preparation methods [27,30,31]. Previous small angle X-ray scattering (SAXS) studies of Nafion–titanate composites prepared by casting evidenced that titanate nanotubes are agglomerated, constituting a segregated phase inside the Nafion matrix [26,30]. On the other hand, nanotubes crystallized *in situ* into Nafion are finely distributed within the polymer bulk [27]. The distribution of nanotubes in the sol–gel composites results in a more effective interaction between the inorganic phase and the hydrophilic phase of Nafion.

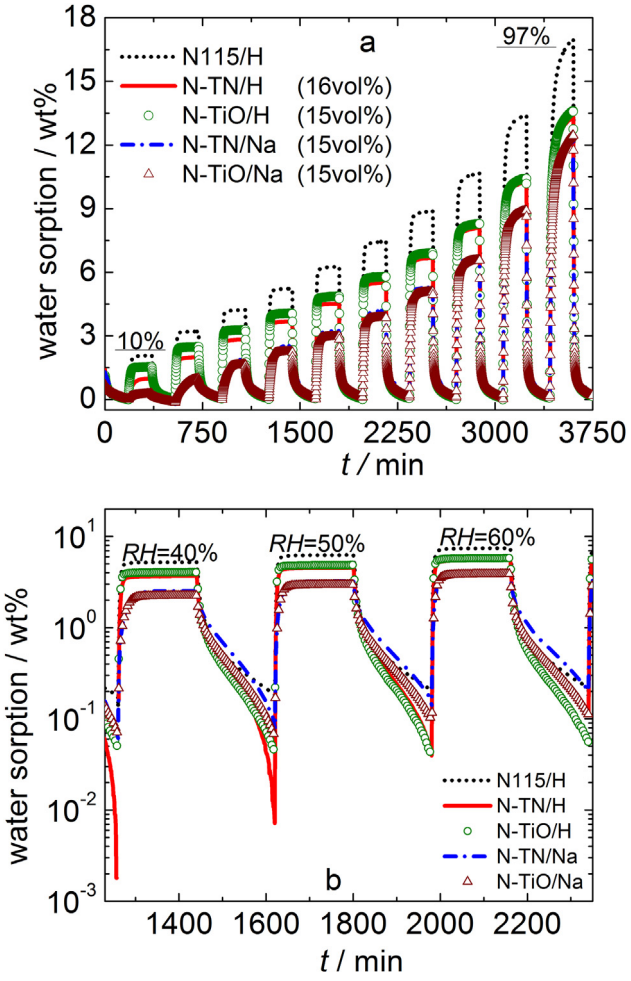

Fig. 2 – (a) Dynamic vapor sorption curves of N–TiO and N-TN composites in the proton and sodium forms at $T = 25\ ^{\circ}C$. The DVS curves for Nafion 115 (proton form) are also shown. (b) Expanded view of the water sorption curve showing three representative relative humidity steps.

The water uptake properties of the composites were studied by dynamic vapor sorption (DVS). Fig. 2 shows the sorption/desorption profiles recorded at $T = 25\ ^{\circ}C$ for Nafion 115, Nafion-TiO_2, and Nafion–titanate nanotubes (*in situ*) in both the proton and sodium forms. Fig. 2a shows the time dependence of the membrane water sorption and desorption at 25 °C with step-like increments of the relative humidity. At low relative humidity ($RH < 80\%$) the water sorption is characterized by a steep increase followed by a plateau at longer measuring times. For $RH > 80\%$, the water sorption requires longer times to reach a maximum value and the equilibrium plateaus are not observed. N115 has the highest water sorption capacity in the entire relative humidity range. The differences between the water uptake of N–TiO and N-TN are negligible, either in the proton or in the sodium forms, being further reduced as the relative humidity increases. The water uptake of ionomers is dependent on the equilibrium between the electrostatic forces among solvated charges, the osmotic pressure of the counterions, and the elastic deformation of the polymer chains [8,32]. The decrease of the water sorption capacity of the *in situ* N-TN composites can be associated with the localization of the nanoparticles in the nanophase-separated morphology of the ionomer. SAXS measurements evidenced that there is an interface between Nafion's hydrophilic phase and the inorganic particles for *in situ* N-TN composites [31]. Such interface may reduce the available sites for water sorption in the ionomer matrix and consequently reduce the water sorption capacity of the composites. Another factor that has to be considered in the water uptake of ionomer membranes is the presence elastic restoring forces that oppose the polymer expansion upon water sorption [8]. The study of the mechanical properties of *in situ* N-TN showed an elastic modulus higher than that of bare Nafion [31]. Such feature indicates that the nanoparticles in the composite samples restrict the motion of the polymer chains and inhibit higher water sorption.

Previous water uptake studies of N-TNcast confirm such hypothesis [30,31]. The elastic modulus of cast composites are lower compared to the ones prepared *in situ* [27]. And as expected, the water sorption of N-TNcast increases with increasing concentration of titanate nanotubes into the ionomer matrix [30,31]. Moreover, the titanate nanotubes are agglomerated in the cast ionomer matrix (N-TNcast) [31]. Both factors contribute to increase the water sorption capacity of the N-TNcast composites.

The expanded view of the time dependence of water sorption shown in Fig. 2b provides information concerning the water retention properties of the composites. For N115, desorption proceeds as a step-like decay of water content at shortened times followed by weaker dependence as time increases. Nonetheless, the desorption curves of all composites exhibit a strong time dependence indicating that the inorganic phase is affecting the water removal from the Nafion hydrophilic phase. In this context, it can be inferred from the desorption curves of Fig. 2b that the N-TN composites in the proton and sodium forms retain higher amounts of water than

the corresponding N–TiO composites. It is assumed that a fraction of the total absorbed water can be retained in the hollow structure of the nanotubes due to capillary condensation [37].

Table 1 shows the diffusion coefficient of water (*D*) calculated from Fig. 2b data (sorption section) using Eq. (1). The water diffusion coefficient of Nafion in both the acid and the sodium forms are in good accordance with the previous reports [8,25]. The diffusion coefficient of water in the composites in the proton form is higher than that in the sodium form, and increases with increasing *RH*. Indeed, *D* in salt neutralized Nafion membranes was shown to decrease with increasing the size of the counterion [32,36], indicating a decrease of the hydrophilic character of the $SO_3^-M^+$ samples.

The increase of *D* with increasing *RH* can be understood as the lowering of the polymer elastic modulus due to the plasticizing effect of water, which favors the water permeation at higher *RH* [32,35]. Interestingly, *D* values for the N-TN/H and N–TiO/H are higher than the one observed for N115/H, a difference more marked at lower RH.

Further evidence of the presence of confined water in N-TN composites is given in Fig. 3. The DSC curves of Nafion display an endothermic minimum at ~ 0 °C associated with the fusion of absorbed water, whereas N-NT/H exhibits two endothermic peaks centered at ~ −1 °C and ~ 7 °C respectively. The presence of two endothermic minima has been reported in DSC scans of mesoporous inorganic particles, being the higher *T* minimum assigned to water confined inside pores, which has its melting point increased due to the capillary condensation [37]. The integrated areas of such endotherms for N115 and N-NT/H are ~ 38 Jg^{-1} and ~ 54 Jg^{-1}, respectively. Such values indicate that titanate nanotubes increased the amount of crystallizable water in the composites.

The DSC curves of Nafion in the dry form display an endothermic minimum (T = 150 °C) associated with a morphological transition occurring due to the destabilization of ionic aggregates [35]. Such transition occurs at higher temperatures (T = 170 °C) in N-TN composites indicating that the interaction of the high aspect ratio nanotubes with the ionomer matrix increases the composite thermal stability, in accordance with previous dynamic mechanical analysis (DMA) [27]. In the wet form the high temperature endothermic peaks of both Nafion and Nafion–titanate are shifted to lower temperatures (~120 °C and ~ 165 °C, respectively). Such a decreased temperature is related to a plasticizing effect of water molecules [35]. Nevertheless, the sharp endothermic

Table 1 – Diffusion coefficient of water molecules (*D*) for Nafion 115 and Nation composites in the proton and sodium forms at different relative humidity.

Film	Diffusion coefficient of water, $D \times 10^{-7}$ [$cm^2\ s^{-1}$]		
	RH = 40%	*RH* = 50%	*RH* = 60%
N115/H	1.19	1.22	1.69
N–TiO/H	1.63	1.71	1.72
N-TN/H	1.45	1.89	1.91
N–TiO/Na	0.27	0.42	0.53
N-TN/Na	0.22	0.29	0.48

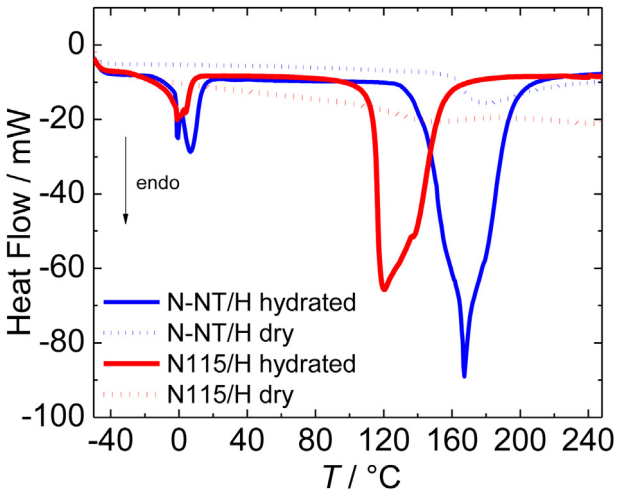

Fig. 3 – Differential scanning calorimetry measurements of Nafion and Nafion titanate nanotubes (~16 vol%) in the hydrated and dry forms.

event occurring at ~165 °C in the hydrated N-TN sample suggests that it can be ascribed to the collapse of the nanotubular structure into rodlike particles as a consequence of the loss of the crystallized water within TiO_6 octaedra [38]. The absence of such endothermic minimum in the dry N-TN composite is in accordance with high-temperature XRD data for titanate nanotubes that showed a high stability of the titanate phase up to ~ 300 °C in dry conditions [39].

The thermal dependence of proton conductivity of N-TN composites was previously evaluated in the 40–130 °C *T*-interval [27]. However, in order to study the ion conductivity of N-TN composites at high *T*, the temperature dependences of the ion conductivity of Nafion, N–TiO and N-TN composites in both sodium and proton forms up to T = 180 °C are shown in Fig. 4.

Similarly to Nafion membranes, the ionic conductivity (σ) of the composite samples (Fig. 4a) follows an Arrhenius-type behavior in the 40–90 °C *T* range and a deviation from the Arrhenius-type temperature dependence for T > 90 °C [33]. However, the N-TN/Hcast sample exhibits distinct temperature dependence. For T > 110 °C the proton conductivity of the cast composite is less sensitive to further increasing *T*, followed by a pronounced s drop at T > 150 °C. The decrease of Σ at high *T* is attributed to a degradation of the cast sample. It has been reported that Nafion membranes immersed in water and conditioned under high *T* and high pressure undergoes a dissolution process [6]. Possibly, the N-TN/Hcast composites were partially dissolved under the conditions of proton conductivity measurements. The lower thermal stability of cast membranes can be a result of the heterogeneous distribution of the inorganic agglomerates that locally disrupts the connectivity of the ionomer chains. In fact, *in situ* N–TiO/H composites revealed to have superior thermomechanical properties compared to cast N–TiO/H [42].

As the water uptake of N-TN and N–TiO (Fig. 2), in both H^+ and Na^+ forms, are similar, the data in Fig. 4 indicate that σ(*T*)

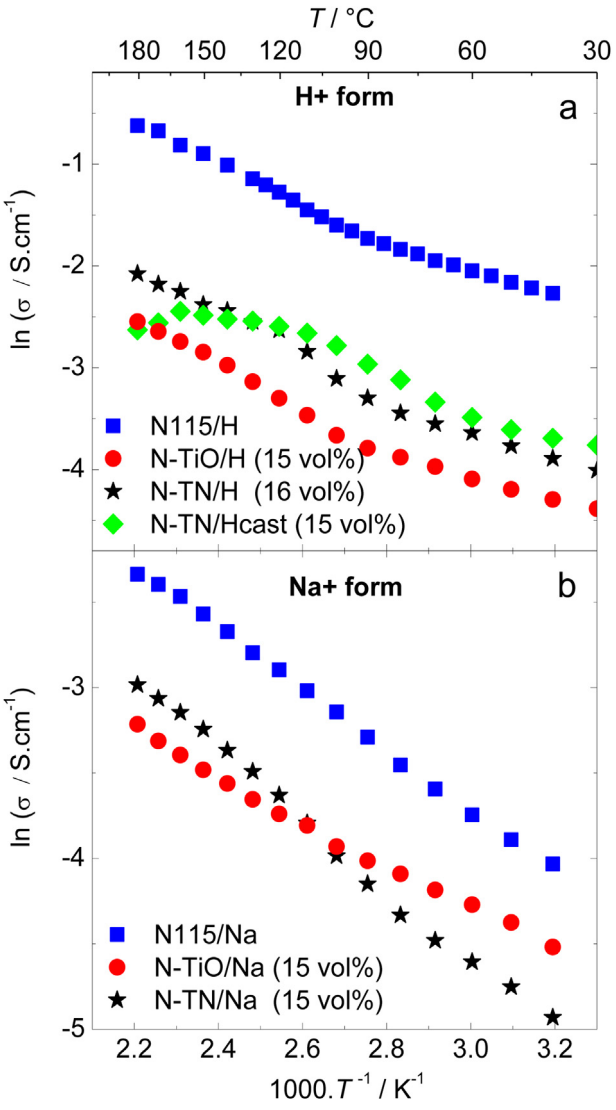

Fig. 4 – Electrical conductivity measurements of Nafion, Nafion–titania and Nafion–titanate nanotubes in the proton (a) and sodium forms (b). The proton conductivity of Nafion–-titanate nanotubes composite prepared by casting is shown for comparison.

values are influenced by the transport properties of the inorganic phase. Previously measured σ of titanate nanotube at *RH* = 100% revealed that the proton conductivity can reach relatively high values (σ ~10^2 S cm^{-1}) [28]. The proton conductivity of N-TN/H composite is higher than that of N–TiO/H in the entire temperature range probably due to the contribution of the ion conducting titanate phase. Similarly, the sodium conductivity of the N-TN/Na composite samples surpasses the one obtained with N–TiO/Na composites at $T > 110$ °C.

The electrical properties of the studied electrolytes are reflected in the performance of DEFC. Fig. 5 shows the temperature dependence of polarization (*I*–*V*) curves and the power density (*p*) curves at $T = 130$ °C of DEFC's using both the *in situ* sol–gel and cast composites.

The *I*–*V* curves obtained in the 80–130 °C *T* range evidenced typical features of DEFC's: i) a large drop of the open circuit voltage (OCV) with respect to the theoretical equilibrium potential for ethanol electro-oxidation (V_{eq} ~ 1.145 V/$T = 25$ °C), and ii) a large polarization loss at low current densities due to activation polarization [2,4,16]. The OCV drop is usually attributed to the crossover of ethanol molecules from the

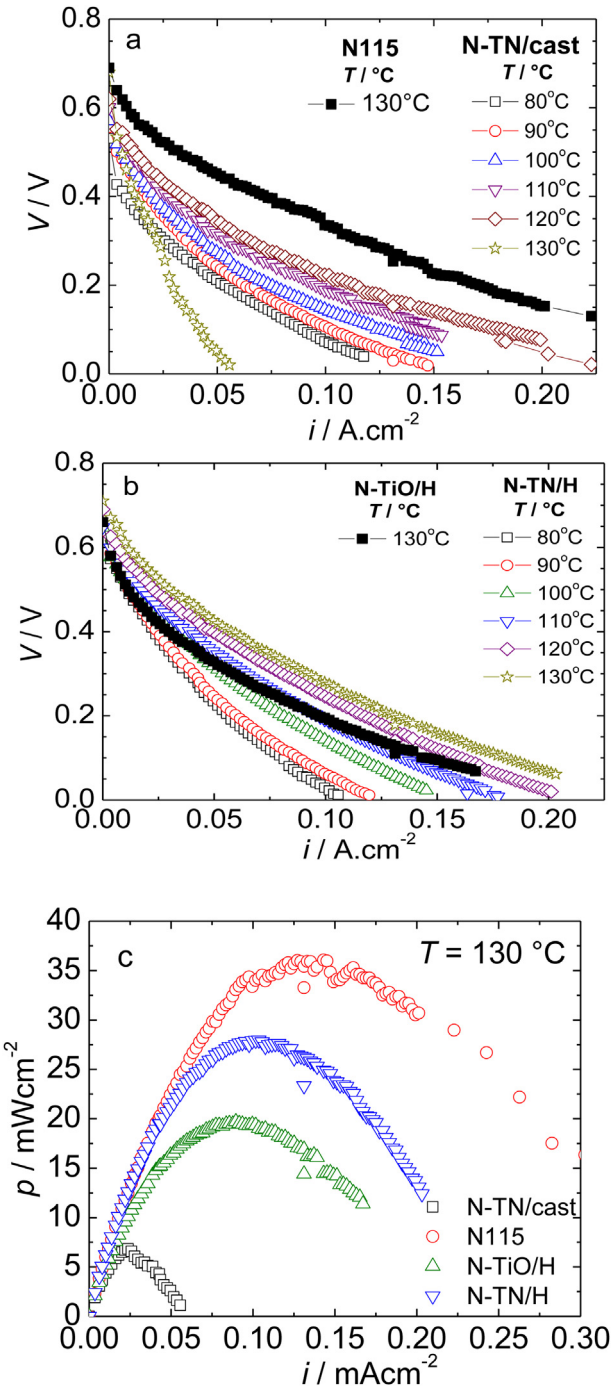

Fig. 5 – Polarization (*I*–*V*) curves of DEFC as a function of temperature for Nafion–titania composites prepared by casting (a) and prepared by *in situ* growth (b). (c) Power density (*p*) for the N115 and Nafion composites at $T = 130$ °C. The *I*–*V* curves of N115 and N–TiO at $T = 130$ °C are shown for comparison.

anode to the cathode, whereas the activation polarization is attributed to the sluggish ethanol oxidation reaction [2]. Thus, taking into account that the studied fuel cells have nominally identical electrodes, the differences observed in the polarization curves, markedly at high current densities, are essentially related to the properties of the composite electrolytes [25]. It can be observed that increasing T increases the DEFC performance using N-TN (Fig. 5b) in the entire temperature range investigated, whereas the DEFC performance using N-TN/cast (Fig. 5a) increased from 80 °C to 120 °C ensued by a dramatic reduction of performance at $T = 130$ °C. The temperature dependence of the DEFC performance and the ohmic drop inferred from the range I–V curves are in good agreement with the temperature dependence of the proton conductivity of the composite electrolytes (Fig. 4). The lower performance of DEFC using N-TN/cast at $T = 130$ °C can be a result of the decreasing conductivity for $T > 110$ °C. Moreover, the lower proton conductivity of N–TiO at $T = 130$ °C resulted in a lower DEFC performance compared to N-TN (Fig. 5b). This feature can be better visualized on Fig. 5c, which shows the power density curves for the Nafion and Nafion composites at $T = 130$ °C.

It can be observed in Fig. 5 that the open circuit voltage (OCV) values of the DEFC using composites are higher for N-TN than those for N-TN/cast. At $T = 130$ °C the OCV increases in the following order: N–TiO (~0.66 V) < N-TN/cast (~0.68 V) < Nafion 115 (~0.69 V) < N-TN (~0.71 V). As the OCV values are mainly associated with the ethanol crossover within the electrolyte, the increment of the OCV strongly indicates the decrease of the ethanol permeability in N-TN electrolytes. Such a feature is in good accordance with the morphological differences existing between the cast and *in situ* prepared composites [27,43]. The preferential localization of the inorganic particles in the hydrophilic phase of Nafion reduces the ethanol crossover and increases the thermal stability of the *in situ* sol–gel N-TN composites.

The fuel crossover in DEFC is responsible for ~50% of the reduction of the DEFC performance [4,5]. Therefore, a reduction of the ethanol crossover promotes the increase of the OCV values and increases the overall DEFC performance. Previous reports evidenced that Nafion composites have higher stability of the DEFC performance at high temperature than pristine Nafion [29]. Thus, the use of Nafion–Titanate Nanotubes composite has the aim of decreasing the ethanol crossover, keeping high proton conductivity values thereby promoting a stable DEFC performance.

Previous reports showed that with further increase in temperature ($T > 130$ °C) the proton conductivity of titanate-nanotubes drops drastically over two orders of magnitude. Such a drop was related to the removal of crystallized water and the destabilization of the nanotube structure that can result in the recrystallization of the inorganic phase into the rutile or anatase structure [38,41]. X-ray diffraction patterns of Nafion–titanate were obtained after proton conductivity measurements up to 180 °C and $RH = 100\%$ as showed in Fig. 6. A crystalline phase transition from the titanate to the rutile phase of titania is observed in the XRD patterns. The recrystallization of the titanate nanotubes into the rutile phase was previously observed to occur in strong acid media, which is in accordance with the chemical environment that the titanate phase is exposed in hydrophilic acid phase of Nafion [41].

The XRD pattern of N-TN/H displays four characteristic peaks at 2θ ~10° (200), 24° (110), 28° (211), and 48° (020) corresponding to the titanate nanotubes, along with the haloes of the polymer matrix [27,39,44]. Such peaks are absent on the XRD pattern of annealed N-TN composite, which exhibits the characteristic peaks of the titania rutile phase [38,39]. In order to study the morphology of rutile nanoparticles, Nafion-rutile composites were dissolved in water and isopropanol mixture at 200 °C in a Teflon-lined autoclave. Representative TEM images of Nafion-Rutile solution were obtained and shown in Fig. 7.

It can be observed in Fig. 7a and b that the titanate nanotubes are converted into titania nanorods. The nanorods are typically ~50–80 nm long with a transverse length of ~10–25 nm, in good accordance with the transverse size of titania rodlike particles prepared by hydrothermal synthesis [40]. A higher magnification (Fig. 7c) evidenced defective planes packing in the internal structure of the nanorods. This feature is an indication that the rutile nanoparticles were collapsed from titanate nanotubes [44]. The titania phase was confirmed by estimating the interplanar distance using XRD data (~0.32 nm) and Fourier Transform (FFT) analysis (~0.32 nm), which correspond to the [110] plane of the rutile structure.

Conclusions

The study of modified Nafion membranes with titanate nanotubes revealed that the electric and electrochemical properties can be further improved by the selection of a suitable synthesis methodology. Nafion–titanate nanotubes prepared by *in situ* sol–gel exhibited improved physicochemical properties with respect to the sample prepared by casting. The synthesis of highly-dispersed titanate nanotubes into Nafion

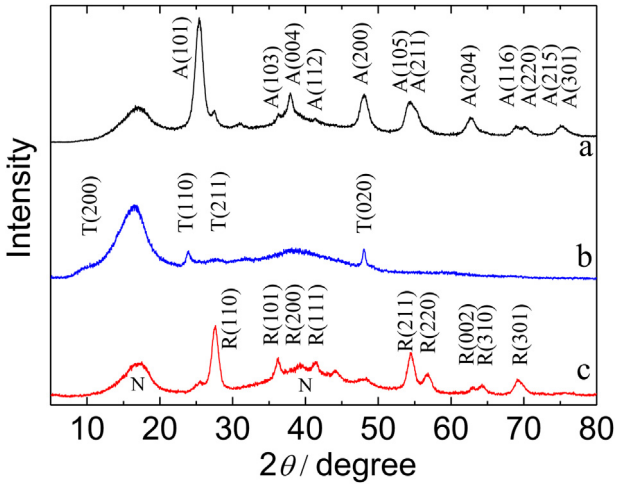

Fig. 6 – X-rays diffraction patterns of Nafion–titania (a) and Nafion–titanate nanotube in the proton form (b) and Nafion–titanate nanotube in the proton form after the conductivity measurements (180 °C) (c). N indicates the characteristic haloes of Nafion, A, T, and R stand for anatase, titanate, and rutile, respectively.

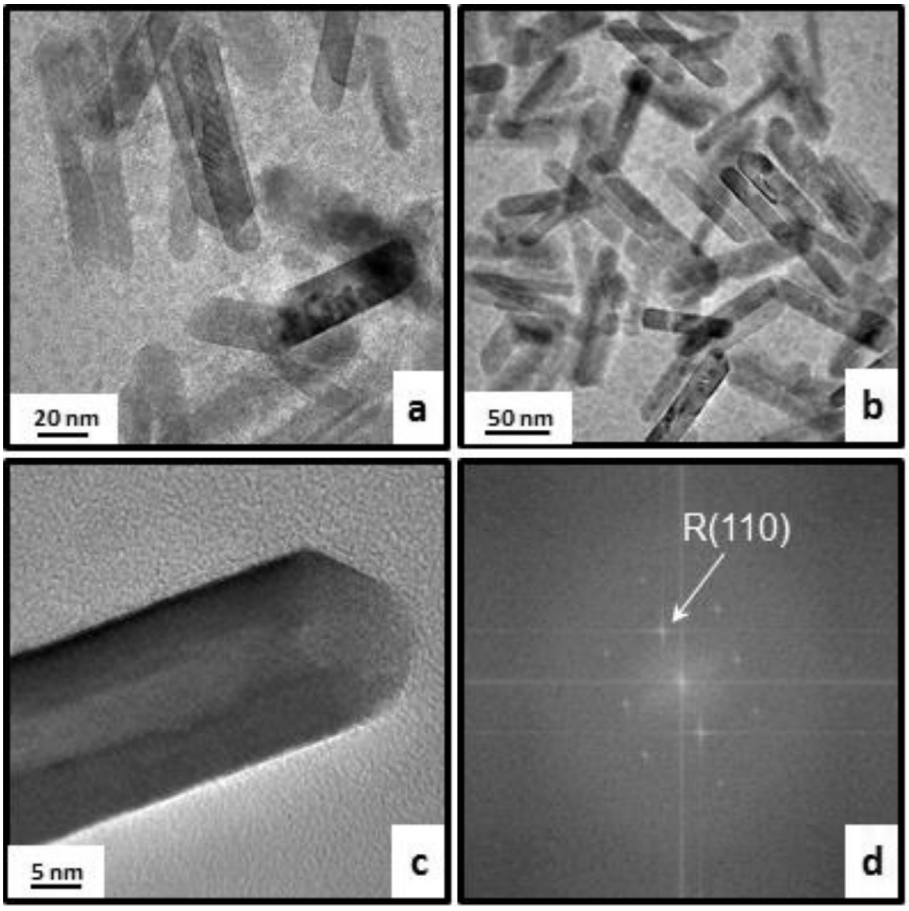

Fig. 7 – (a and b) Representative TEM images of the collapsed rutile nanoparticles formed inside Nafion membranes at high temperatures; (c) high resolution image of a nanorod particle; (d) Fast Fourier transform of Fig. 7c.

membranes was possible due to a microwave-assisted *in situ* conversion of sol–gel titania (anatase) particles. Such a synthesis method ensures a strong interaction between the hydrophilic ionic aggregates of the ionomer matrix and the inorganic phase. However, no significant differences on the water uptake between Nafion–titanate nanotube and Nafion–titania composites were observed, irrespectively to the ability of nanotubes to retain water superficially. The higher conductivity of Nafion–titanate composites as compared to Nafion–titania was shown to be mainly a result of the high proton conductivity of the titanate nanotubes, which is considerably higher than that of anatase nanoparticles. Nafion–titanate composites prepared by casting displayed inferior proton conductivity and DEFC performance at high temperatures. Such properties indicate that Nafion-nanotube nanocomposites prepared by *in situ* crystallization are potential electrolytes for polymer electrolyte fuel cells operating at intermediate temperature ($\leq$130 °C).

Acknowledgments

Thanks are due to the Brazilian funding agencies (CAPES, CNPQ, FAPESP) and also to CNEN. This work was performed with the financial support of the Natural Sciences and Engineering Research Council of Canada and the Canadian Foundation for Innovation.

REFERENCES

[1] Kamarudin MZF, Kamarudin SK, Masdar MS, Daud WRW. Review: direct ethanol fuel cells. Int J Hydrogen Energy 2013;38:9438.
[2] Song S, Tsiakaras P. Recent progress in direct ethanol proton exchange membrane fuel cells (De-Pemfcs). Appl Catal B Environ 2006;63:187.
[3] Zignani SC, Gonzalez ER, Baglio V, Siracusano S, Aricò AS. Investigation of a Pt3Sn/C electro-catalyst in a direct ethanol fuel cell operating at low temperatures for portable applications. Int J Electrochem Sci 2012;7:3155.
[4] Deluca NW, Elabd YA. Polymer electrolyte membranes for the direct methanol fuel cell: a review. J Polym Sci Part B Polym Phys 2006;44:2201.
[5] Ahmed M, Dincer I. A review on methanol crossover in direct methanol fuel cells: challenges and achievements. Int J Energy Res 2011;35:1213.
[6] Kreuer K-D. The role of internal pressure for the hydration and transport properties of ionomers and polyelectrolytes. Solid State Ionics 2013;252:93.

[7] Li J, Park JK, Moore RB, Madsen LA. Linear coupling of alignment with transport in a polymer electrolyte membrane. Nat Mater 2011;10:507.
[8] Majsztrik PW, Satterfield MB, Bocarsly AB, Benziger JB. Water sorption, desorption and transport in nafion membranes. J Mem Sci 2007;301:93.
[9] Kreuer K-D. Proton conductivity: materials and applications. Chem Mater 1996;8:610.
[10] Matos BR, Dresch MA, Santiago EI, Linardi M, de Florio DZ, Fonseca FC. Nafion β-relaxation dependence on temperature and relative humidity studied by dielectric spectroscopy. J Electrochem Soc 2013;160:F43.
[11] Young SK, Trevino SF, Beck-Tan NC. Small-angle neutron scattering investigation of structural changes in nafion membranes induced by swelling with various solvents. J Polym Sci Part B Polym Phys 2002;40:387.
[12] Vigier F, Coutanceau C, Perrard A, Belgsir EM, Lamy C. Development of anode catalysts for a direct ethanol fuel cell. J Appl Electrochem 2004;34:439.
[13] Mann J, Yao N, Bocarsly AB. Characterization and analysis of new catalysts for a direct ethanol fuel cell. Langmuir 2006;22:10432.
[14] Colmati F, Antolini E, Gonalez ER. Ethanol oxidation on carbon supported Pt-Sn electrocatalysts prepared by reduction with formic acid. J Electrochem Soc 2007;154:B39.
[15] Linares JJ, Zignani SC, Rocha TA, Gonzalez ER. Ethanol oxidation on a high temperature PBI-based DEFC using Pt/C, PtRu/C and Pt_3Sn/C as catalysts. J Appl Electrochem 2013;43:147.
[16] Linares JJ, Rocha TA, Zignani S, Paganin VA, Gonzalez ER. Different anode catalyst for high temperature polybenzimidazole-based direct ethanol fuel cells. Int J Hydrogen Energy 2013;38:620.
[17] Zhang J, Xie Z, Zhang J, Tang Y, Song C, Navessin T, et al. High temperature PEM fuel cells. J Power Sources 2006;160:872.
[18] Liu G, Zhang H, Hu J, Zhai Y, Xu D, Shao Z-g. Studies of performance degradation of a high temperature PEMFC based on H_3PO_4-doped PBI. J Power Sources 2006;162:547.
[19] Haile SM, Boysen DA, Chisholm CRI, Merle RB. Solid acids as fuel cell electrolytes. Nature 2001;410:910.
[20] Boysen DA, Uda T, Chisholm CRI, Haile SM. High-performance solid acid fuel cells through humidity stabilization. Science 2004;303:68.
[21] Suresh NS, Jayanti S. Cross-over and performance modeling of liquid-feed polymer electrolyte membrane direct ethanol fuel cells. Inter J Hydrogen Energy 2011;36:14648.
[22] Song SQ, Zhou WJ, Zhou ZH, Jiang LH, Sun GQ, Xin Q, et al. Direct ethanol PEM fuel cells: the case of platinum based anodes. Inter. J Hydrogen Energy 2005;30:995.
[23] Tseng C-Y, Ye Y-S, Kao K-Y, Joseph J, Shen W-C, Rick J, et al. Interpenetrating network-forming sulfonated poly(vinyl alcohol) proton exchange membranes for direct methanol fuel cell applications. Inter. J Hydrogen Energy 2011;36:11936.
[24] Fu R-Q, Hong L, Lee J-Y. Membrane design for direct ethanol fuel cells: a hybrid proton-conducting interpenetrating polymer network. Fuel Cells 2008;8:52.
[25] Mecheri B, Felice V, Zhang Z, D'Epifanio A, Licoccia S, Tavares AC. DSC and DVS investigation of water mobility in nafion/zeolite composite membranes for fuel cell applications. J Phys Chem C 2012;116:20820.
[26] Alberti G, Casciola M. Composite membranes for medium-temperature PEM fuel cells. Annu Rev Mater Res 2003;33:129.
[27] Matos BR, Isidoro RA, Santiago EI, Linardi M, Ferlauto AS, Tavares AC, et al. *In situ* fabrication of nafion–titanate hybrid electrolytes for high-temperature direct ethanol fuel cell. J Phys Chem C 2013;117:16863.
[28] Kasuga T. Formation of titanium oxide nanotubes using chemical treatments and their characteristic properties. Thin Solid Films 2006;496:141.
[29] Santiago EI, Isidoro RA, Dresch MA, Matos BR, Linardi M, Fonseca FC. Nafion–TiO_2 hybrid electrolytes for stable operation of PEM fuel cells at high temperature. Electrochim Acta 2009;54:4111.
[30] Matos BR, Santiago EI, Fonseca FC, Linardi M, Lavayen V, Lacerda RG, et al. Nafion–titanate nanotube composite membranes for PEMFC operating at high temperature. J Electrochem Soc 2007;154:B1358.
[31] Matos BR, Santiago EI, Rey JFQ, Ferlauto AS, Traversa E, Linardi M, et al. Nafion-based composite electrolytes for proton exchange membrane fuel cells operating above 120 °C with titania nanoparticles and nanotubes as fillers. J Power Sources 2011;196:1061.
[32] Takamatsu T, Hashiyama M, Eisenberg A. Sorption phenomena in nafion membranes. J Appl Polym Sci 1979;24:2199.
[33] Matos BR, Andrade CA, Santiago EI, Fonseca FC. Proton conductivity of perfluorosulfonate ionomers at high temperature and high relative humidity. Appl Phys Lett 2014;104:091904.
[34] Bavykin DV, Friedrich JM, Walsh FC. Protonated titanates and TiO_2 nanostructured materials: synthesis, properties, and applications. Adv Mater 2006;18:2807.
[35] Kyu T, Eisenberg A. Underwater stress relaxation studies of nafion (perfluorosulfonate) ionomer membranes. J Polym Sci Polym Symp 1984;71:203.
[36] Dugas R, Guay D, Tavares AC. Simultaneous determination of the permeability of a nafion membrane to formic acid and water. Fuel Cells 2013;13:1024.
[37] Kittaka S, Ueda Y, Fujisaki F, Iiyama T, Yamaguchi T. Mechanism of freezing of water in contact with mesoporous silicas MCM-41, SBA-15 and SBA-16: role of boundary water of pore outlets in freezing. Phys Chem Chem Phys 2011;13:17222.
[38] Thorne A, Kruth A, Tunstall D, Irvine JTS, Zhou W. Formation, structure, and stability of titanate nanotubes and their proton conductivity. J Phys Chem B 2005;109:5439.
[39] Morgado Jr E, de Abreu MAS, Moure GT, Marinkovic BA, Jardim PM, Araujo AS. Characterization of nanostructured titanates obtained by alkali treatment of TiO_2-anatases with distinct crystal sizes. Chem Mater 2007;19:665.
[40] Lan Y, Gao X, Zhu H, Zheng Z, Yan T, Wu F, et al. Titanate nanotubes and nanorods prepared from rutile powder. Adv Func Mater 2005;15:1310.
[41] Zhu HY, Lan Y, Gao XP, Ringer SP, Zheng ZF, Song DY, et al. Phase transition between nanostructures of titanate and titanium dioxides via simple wet-chemical reactions. J Am Chem Soc 2005;127:6730.
[42] Matos BR, Arico EM, Linardi M, Ferlauto AS, Santiago EI, Fonseca FC. Thermal properties of nafion–TiO_2 composite electrolytes for PEM fuel cell. J Therm Anal Calorim 2009;97:591.
[43] Matos BR, Isidoro RA, Santiago EI, Fonseca FC. Performance enhancement of direct ethanol fuel cell using nafion composites with high volume fraction of titania. J Power Sources 2014;268:706.
[44] Morgado Jr E, de Abreu MAS, Pravia ORC, Marinkovic BA, Jardim PM, Rizzo FC, et al. A study on the structure and thermal stability of titanate nanotubes as a function of sodium content. Solid State Sci 2006;8:888.